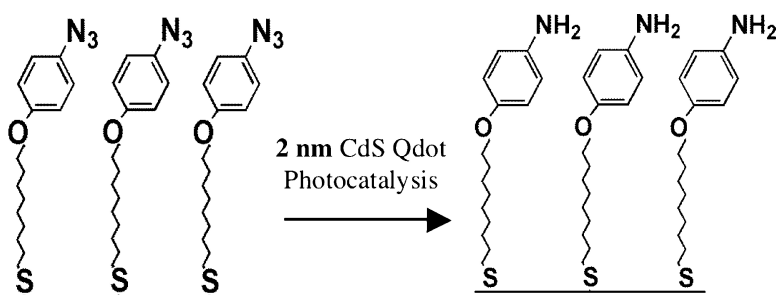


## Photocatalytic Reduction of an Azide-Terminated Self-Assembled Monolayer Using CdS Quantum Dots

Chander Radhakrishnan, Michael K. F. Lo, Manoj V. Warriar, Miguel A. Garcia-Garibay, and Harold G. Monbouquette

*Langmuir*, 2006, 22 (11), 5018-5024 • DOI: 10.1021/la060035y

Downloaded from <http://pubs.acs.org> on February 6, 2009



### More About This Article

Additional resources and features associated with this article are available within the HTML version:

- Supporting Information
- Links to the 2 articles that cite this article, as of the time of this article download
- Access to high resolution figures
- Links to articles and content related to this article
- Copyright permission to reproduce figures and/or text from this article

[View the Full Text HTML](#)

## Photocatalytic Reduction of an Azide-Terminated Self-Assembled Monolayer Using CdS Quantum Dots

Chander Radhakrishnan,<sup>†</sup> Michael K. F. Lo,<sup>†</sup> Manoj V. Warriar,<sup>†</sup>  
Miguel A. Garcia-Garibay,<sup>\*,‡,§</sup> and Harold G. Monbouquette<sup>\*,†,§</sup>

Chemical and Biomolecular Engineering Department, University of California, Los Angeles, Los Angeles, California 90095-1592, Department of Chemistry and Biochemistry, University of California, Los Angeles, Los Angeles, California 90095-1569, and California NanoSystems Institute, University of California, Los Angeles, Los Angeles, California 90095

Received January 4, 2006. In Final Form: March 7, 2006

Ordered, tightly packed aryl-azide-terminated, self-assembled monolayers (SAMs) were created on gold substrates from a new disulfide precursor. These monolayers were reduced at least partially in an aqueous environment using ~2 nm CdS quantum dots (Qdots) as photocatalysts to give mixed monolayers of arylamine- and aryl azide-terminated species. The CdS photocatalysts were made available for the reaction by exposure of the azide-terminated SAM to Qdots initially in solution or by preadsorption of the CdS nanoparticles on the SAM. In either case, X-ray photoelectron spectroscopy (XPS), grazing angle Fourier transform infrared spectroscopy (FTIR), and contact angle measurements were used to show the occurrence of the photocatalytic reduction. As further evidence for the presence of arylamine-terminated thiolate in the reduced SAM, these arylamine groups were successfully tagged with fluorescein isothiocyanate (FITC). The use of Qdot photocatalysts to functionalize surfaces may lead to a means to pattern surfaces at the nanoscale.

### Introduction

Semiconductor nanoparticles of sizes less than the corresponding bulk exciton diameter are known as quantum dots (Qdots) and have become an important focus of research due to their quantum confinement behavior, which is manifested in size-tunable optoelectronic properties.<sup>1,2</sup> One significant and readily observable effect is the shift of the onset of absorption to shorter wavelengths (indicating increased band gap) with decreasing Qdot diameter. Qdots, especially II–VI materials, have been explored extensively for applications in light emitting devices<sup>3</sup> and in solar energy conversion.<sup>4</sup> Qdots can also be versatile photocatalysts,<sup>5–7</sup> as their electron–hole potentials can be tuned through manipulation of particle size. By ensuring a high surface-to-volume ratio and reduced trap concentration, the photoexcited electrons and holes can be made readily available at the Qdot surface for reduction or oxidation of adsorbed species, respectively. Increased photooxidation/reduction rates have been observed previously with MoS<sub>2</sub>,<sup>8</sup> PbSe,<sup>9</sup> TiO<sub>2</sub>,<sup>10</sup> In<sub>2</sub>S<sub>3</sub>,<sup>11</sup> ZnO,<sup>12</sup>

and CdS<sup>13–15</sup> nanoparticle photocatalysts in solution. Although Qdots have been shown to be efficient photocatalysts in homogeneous solution and charge-transfer mechanisms and rates have been well documented, they have not been used to drive photocatalytic reactions on surfaces.<sup>10,11,13–15</sup> In our earlier work, we showed that CdS and CdSe Qdots can act as highly chemoselective photocatalysts for the reduction of aryl azides to the corresponding arylamines in homogeneous solution.<sup>16</sup> A reaction mechanism was postulated, and the quantum yields were experimentally determined to be almost 50%. The high efficiency of the Qdot photocatalyzed reduction is attributed to the large driving force for electron transfer to the azide, which in turn arises from the much more negative potential of excited Qdot electrons (−1.7 V vs NHE for 2 nm CdS Qdots)<sup>15</sup> relative to the azide (*p*-nitrophenyl azide) reduction potential (−0.59 V vs NHE).<sup>17</sup> In this paper, we report the reduction of aryl azide-terminated, self-assembled monolayers (SAMs) on gold to the corresponding arylamine species using CdS Qdots as photocatalysts. A pictorial representation of our azide SAM reduction scheme is shown (Scheme 1A) along with a simplified model for the actual redox process (Scheme 1B). By using Qdot photocatalysis, it may be feasible to obtain chemically modified patterns on an azide-terminated SAM by adsorbing Qdot photocatalysts in a pre-defined arrangement followed by photocatalytic reduction and chemical derivatization. Further, as the surface group reaction is Qdot mediated, the pattern feature dimensions potentially could be reduced to the size of the Qdot itself, thereby providing a route to creation of defined surface patterns at the nanometer scale.

\* To whom correspondence should be addressed. (H.G.M.) E-mail: hmonbouq@ucla.edu. Tel: 310-825-8946. Fax: 310-206-4107. (M.A.G.-G.) E-mail: mgg@chem.ucla.edu. Tel: 310-825-3159. Fax: 310-825-0767.

<sup>†</sup> Chemical and Biomolecular Engineering Department.

<sup>‡</sup> Department of Chemistry and Biochemistry.

<sup>§</sup> California NanoSystems Institute.

(1) (a) Berry, C. R. *Phys. Rev.* **1967**, *161*, 848. (b) Brus, L. E. *J. Phys. Chem.* **1986**, *90*, 2555.

(2) Steigerwald, M. L.; Brus, L. E. *Annu. Rev. Mater. Sci.* **1988**, *19*, 471.

(3) Colvin, V. L.; Schlamp, M. C.; Alivisatos, A. P. *Nature* **1994**, *370*, 354.

(4) Huang, Z. Y.; Barber, T.; Mills, G.; Morris, M. B. *J. Phys. Chem.* **1994**, *98*, 12746.

(5) Fox, M. A.; Dulay, M. T. *Chem. Rev.* **1993**, *93*, 341.

(6) Anders, H.; Grätzel, M. *Chem. Rev.* **1995**, *95*, 49.

(7) Serpone, N.; Pelizzetti, E. *Photocatalysis*; Wiley: New York, 1989.

(8) Thurston, T. R.; Wilcoxon, J. P. *J. Phys. Chem. B.* **1999**, *103*, 11.

(9) Nedeljković, J. M.; Nenadović, M. T.; Micić, O. I.; Nozik, A. J. *J. Phys. Chem.* **1986**, *90*, 12.

(10) Brown, G. T.; Darwent, J. R.; Fletcher, P. D. I. *J. Am. Chem. Soc.* **1985**, *107*, 6446.

(11) Nosaka, Y.; Ohta, N.; Miyama, H. *J. Phys. Chem.* **1990**, *94*, 3752.

(12) Hoffman, A. J.; Hoffman, M. R. In *Photocatalytic Purification and Treatment of Water and Air*; Ollis, D. F., Al-Ekabi, H., Eds.; Elsevier Science Publishers B. V.: Amsterdam, 1993; pp 155–162.

(13) Matsumoto, H.; Uchida, H.; Matsunaga, H.; Tanaka, K.; Sakata, T.; Mori, H.; Yoneyama, H. *J. Phys. Chem.* **1994**, *98*, 11549.

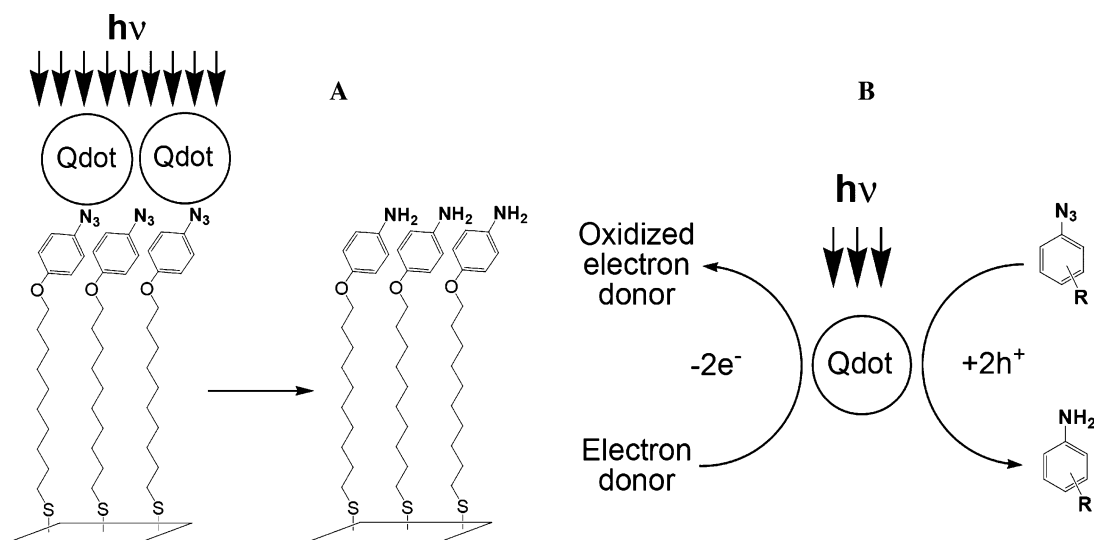
(14) Rossetti, R.; Brus, L. E. *J. Phys. Chem.* **1986**, *90*, 558.

(15) Korgel, B. A.; Monbouquette, H. G. *J. Phys. Chem. B.* **1997**, *101*, 5010.

(16) Warriar, M.; Lo, M. K. F.; Monbouquette, H. G.; Garcia-Garibay, M. A. *Photochem. Photobiol. Sci.* **2004**, *3*, 859.

(17) Herbranson, D.; Hawley, M. *J. Org. Chem.* **1990**, *55*, 4297.

**Scheme 1. (A) Reduction of Aryl Azide SAM to Arylamine Using CdS Qdot Photolysts and (B) a Simplified Model of Qdot Mediated Redox Process**



### Experimental Section

**Chemicals.** All chemicals were purchased from Acros unless indicated otherwise. Cadmium chloride 99.99+%, sodium sulfide nonahydrate 99.99+%, 2-(*N,N*-diethylamino)ethanethiol hydrochloride 96%, sodium formate 99%, benzene  $\geq 99.5\%$  (Aldrich), triethanolamine 99.7%, fluorescein isothiocyanate (FITC) 90% (isomer 1), methanol 99.8%, triphenylphosphine 99%, tetrahydrofuran (extra dry), and guanidine hydrochloride (99%) all were used fresh and without further purification. Aryl azide disulfides were synthesized in our lab (see the Supporting Information).

**Procedures. CdS Nanoparticles Synthesis.** CdS nanocrystals were synthesized at room temperature in water using an arrested growth method with 2-(*N,N*-diethylamino)ethanethiol hydrochloride as a colloidal stabilizer.<sup>16</sup> Deionized water (200 mL, 18 M $\Omega$ ) was sparged with ultrahigh purity argon for 60 min. To 150 mL of the argon-sparged water was added 27.5 mg of CdCl<sub>2</sub> (0.15 mM) along with 398 mg of tertiary amine thiol (3.5 mM). The pH of this clear mixture was adjusted to 7.0 by dropwise addition of 1 M NaOH. In a separate flask, 60 mg (0.25 mM) of Na<sub>2</sub>S was dissolved in 25 mL of argon-sparged water and transferred dropwise to the cadmium chloride solution. The solution turned pale yellow immediately after sulfide addition. The resulting nanoparticle size depended on both the pH prior to sulfide addition and on the molar ratio of cadmium precursor to tertiary amine thiol capping agent. The synthesized nanocrystals were characterized (UV-visible absorption and emission spectra at 380 nm excitation) and then stored under argon in the dark.

**Substrate Preparation.** The gold substrates for SAM deposition were prepared by electron beam evaporation of a 2.5 nm chromium adhesion layer (1 Å/s) followed by 50 nm of gold (3 Å/s) at 10<sup>-6</sup>–10<sup>-7</sup> Torr onto 4 in. silicon (100) wafer (Silicon Quest International). The deposition was carried out at room temperature. Previous studies have established that this procedure produces polycrystalline gold films with (111) orientation and grain size in excess of 1000 Å.

**SAM Preparation.** The gold-coated wafers were diced into 1 × 1 cm pieces and were immersed in hot piranha solution (~90 °C) for 10 min and then washed extensively in flowing DI water. (Caution: Piranha is a mixture of 30% hydrogen peroxide solution and concentrated sulfuric acid (98%) in the ratio of 1:3. Great care must be taken while handling piranha solution, as it has been known to detonate spontaneously on contact with organics.) The samples were ultrasonicated in HPLC grade acetone for 2 min and dried thoroughly in argon. A 1 mM solution of freshly synthesized aryl azide functionalized disulfide precursor (see Scheme 2 and the Supporting Information) was prepared in dry benzene, and the cleaned gold substrates were left immersed in it in a dark, argon-purged glovebox. After 24 h, the samples were removed and ultrasonicated, first in benzene and then DI water for 30 s each to remove any

physisorbed layers or oxidized species. These aryl azide SAMs on gold finally were dried and stored under argon in the dark.

**Photocatalytic Reduction with Qdots Initially Free in Solution.** A total of 10 mL of freshly synthesized CdS Qdot solution in water (pH 7.0) was mixed with 5 mL of 200 mM sodium formate aqueous solution in a 20 mL Pyrex vial with a PTFE septum cap. During photocatalysis, the formate played the important role of sacrificial electron donor to the excited hole on the CdS Qdot. The aryl azide SAM on gold was placed in the vial, purged with argon, and then housed in a small box, which was wrapped in aluminum foil except for a 5 × 5 cm opening. (The argon purging was carried out to minimize photooxidation of both the Qdot thiol capping agent and the gold thiolate bond during photocatalysis.) A 400 nm cutoff filter (Edmund Optics) was placed over the 5 × 5 cm opening to suppress direct photolysis of the aryl azide. A water jacket was used to filter off IR radiation, and an additional heat absorbing glass (Edmund Optics) was placed on top of the UV cutoff filter to avoid any heating of the vial contents. Irradiation of the sample was carried out for 2 h using a 400 W Hanovia arc lamp. Subsequently, the SAM sample was ultrasonicated in DI water for 30 s, dried and stored under argon in the dark.

**Photocatalytic Reduction with Preadsorbed Qdots.** Aryl azide SAM samples were placed in argon-purged vials containing fresh CdS Qdot solution (pH 7.0) and exposed for 12 h to allow for Qdot adsorption. The SAM coated samples were subsequently removed, rinsed in acidified DI water (pH 6), and stored in a Pyrex vial containing 200 mM sodium formate solution. The setup and conditions used for photolysis were the same as those described above. After photolysis, the SAM sample was ultrasonicated in DI water for 30 s, dried, and stored under argon in the dark.

**Chemical Reduction using Triphenylphosphine.** Aryl azide-terminated SAM samples were left in the dark in a stirred 0.01 M solution of triphenylphosphine (Ph<sub>3</sub>P) in dry THF for 2 days. The SAM sample then was removed and placed in stirred DI water for 2 h. Finally, the SAM was ultrasonicated in THF and DI water for 30 s each, dried under argon, and stored in the dark until characterization.

**Fluorescein Isothiocyanate (FITC) Derivatization.** The arylamine moiety generated by reducing the azide SAM was subjected to a covalent tagging reaction using FITC.<sup>18</sup> The reduced SAM sample was dipped in a triethylamine (TEA)-dry dichloromethane mixture (1:4) to deprotonate the amine and was immediately transferred to a reaction vessel containing 1 mg of FITC in 10 mL of dry methanol (with 25  $\mu$ L of TEA). A micro stir bar was used to stir the reaction

(18) Imhof, A.; Megens, M.; Engelberts, J. J.; de Lang, D. T. N.; Sprik, R.; Vos, W. L. *J. Phys. Chem. B* **1999**, *103*, 1408.

mixture in the dark under a blanket of argon. After 30 min, the SAM was removed from the reaction vessel and washed with excess methanol to remove noncovalently bound dye. The SAM then was dried in argon and stored in the dark until characterization.

**Instrumentation.** *UV-vis and Emission Spectroscopy.* Optical absorption spectra of CdS nanocrystal solutions at room temperature were obtained using a commercial UV-vis spectrometer (Ocean Optics Inc.) The emission spectra (400–750 nm at 380 nm excitation) for the same solutions were obtained using a fluorometer in right angle mode (Jobin-Yvon Spex Fluorolog). FITC derivatized SAMs were mounted on a surface sample stage and were excited at 450 nm. The emission spectra between 475 and 650 nm were recorded in the front face mode (the mount was tilted at a shallow angle of  $11^\circ$  to the normal to avoid scattering noise<sup>19</sup>).

*Fourier Transformed Infrared Spectroscopy (FTIR).* IR spectra of the aryl azide-functionalized disulfides (KBr) were obtained using a single-beam spectrometer (Beckman Paragon 1000). Spectra were recorded at  $4\text{ cm}^{-1}$  resolution and were averaged over 16 scans. Reflection IR absorption spectra of SAMs were obtained with a Digilab FTS 175C single beam spectrometer fitted with an MCT detector and custom optics optimized for grazing angle incidence reflection ( $85^\circ$ ). The sample compartment of the spectrometer was purged constantly with nitrogen to prevent water vapor interference. Freshly cleaned bare gold substrates were used to obtain background spectra. All reflectance spectra were recorded at  $4\text{ cm}^{-1}$  resolution and averaged over 1024 scans.

*Contact Angle.* Contact angles were measured with an FTÅ 4000 Microdrop contact angle goniometer (First Ten Ångströms, Portsmouth, VA). This instrument was equipped with a microliter syringe whose Z position was software controlled. The sessile drop method was used throughout, wherein a droplet of water ( $5\ \mu\text{L}$ ) was formed on the end of the syringe and lowered onto the surface. The syringe was then retracted until the drop detached itself. Three measurements per sample were made at different points on the sample. All angles were quoted as the means ( $n \geq 3$ ) with standard error.

*X-ray Photoelectron Spectroscopy (XPS).* XPS data were taken with a Kratos Axis Ultra spectrometer using monochromated Al K $\alpha$  radiation at 1486.6 eV and normal escape angle. The source was operated at 225 W. Survey scans were taken at 160 eV pass energy and high-resolution scans at 20 or 40 eV pass energy. Peaks were referenced to Au 4f<sub>7/2</sub> at 84.0 eV. The S2p, N1s, and Cd3d peaks were fit with mixed Gaussian/Lorentzian profile peak shapes after subtraction of a Shirley-type background.<sup>20</sup>

*Electrochemistry.* Cyclic voltammetry was performed with an EG&G Instruments potentiostat/galvanostat model 283 (Perkin-Elmer Instrument, Atlanta, TX). All potentials were reported versus the Ag|AgCl reference electrode unless indicated otherwise. The K<sub>4</sub>Fe(CN)<sub>6</sub>/K<sub>3</sub>Fe(CN)<sub>6</sub> redox couple was used as the electrochemical probe in 100 mM phosphate buffer. A gold electrode with an active area of  $2\text{ mm}^2$  was modified with the aryl azide-terminated monolayer and was used as the working electrode. The potential was scanned from  $-0.6$  to  $+0.6\text{ V}$  at a rate of  $100\text{ mV/s}$ .

## Results and Discussion

**CdS Qdot Synthesis and Characterization.** Since Qdot size directly affects exciton energies and electron-hole redox properties, it is essential to control well the size of these photocatalytic nanoparticles. Although several different protocols have been established to obtain nanoparticles, a simple colloidal arrested-growth technique was adopted to synthesize CdS Qdots in water at room temperature.<sup>15,21</sup> CdCl<sub>2</sub> and Na<sub>2</sub>S·9H<sub>2</sub>O were used as precursors with 2-(*N,N*-diethylamino)ethanethiol hydrochloride as the size-regulating and surface-stabilizing ligand. Use of the tertiary aminethiol capping ligand was preferred over aminoethanethiol, as it resulted in narrower Qdot size distribu-

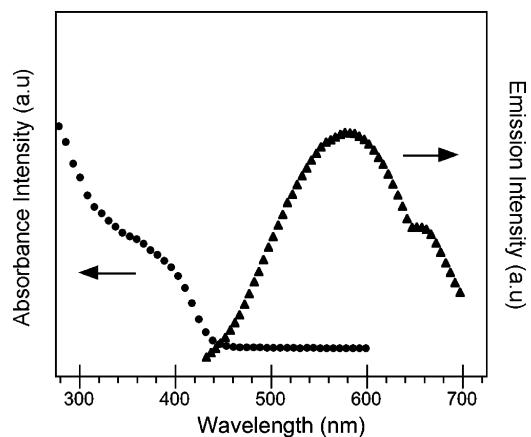
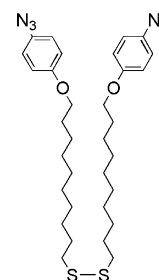


**Figure 1.** UV-vis absorption (●) and emission spectra (▲) of CdS Qdots synthesized in water.

### Scheme 2. Aryl Azide Disulfide (SAM Precursor)



tions. The normalized UV-vis absorption and emission spectra of fresh Qdots are shown in Figure 1. The Qdot diameter as synthesized was estimated to be  $\sim 2.1\text{ nm}$  based on a correlation of the exciton energy (approximated from absorption spectra) with the nanoparticle size using the empirical pseudopotential model (EPM) for hexagonal CdS Qdots.<sup>22</sup> However, a TEM image (not shown) suggested prolate Qdots with average dimensions of  $2.3 \pm 0.2$  and  $3.1 \pm 0.2\text{ nm}$  for the short and long axes, respectively. Larger Qdots were obtained by refluxing under argon for 10 min or more, although Qdots of increased size generated by refluxing always resulted in a broader size distribution. Smaller Qdots are preferred over larger Qdots for azide photocatalysis due to inherently more negative excited electron potentials. The Qdot emission spectrum has a broad peak centered around 540 nm suggesting deep trap emission. This is expected in very small Qdots and is attributed to incomplete surfaces (missing surface atoms) leading to surface defects that can act as recombination centers.<sup>23</sup> Trap emission is not expected to eliminate photocatalytic activity, as charge transfer is known to occur somewhat faster ( $\sim 20\text{ ps}$ )<sup>24</sup> than electron hole recombination ( $\sim 40\text{ ps}$ ).<sup>14</sup> Moreover, Qdots previously produced in the same manner were shown to be very efficient in photocatalyzing aryl azide reduction in solution.<sup>16</sup>

**Aryl Azide-Terminated SAM Characterization.** Aryl azide SAMs were assembled on smooth gold substrates from the disulfide precursor (Scheme 2). This particular aryl azide was chosen for the high ( $\sim 30\%$ ) quantum yield for the CdS Qdot photocatalyzed reduction in solution and the reactivity of the resulting primary arylamine. Although an alkyl azide SAM would be preferred for post reduction derivatization, the required disulfide precursor could not be synthesized easily with high

(19) Fox, M. A.; Whitesell, J. K.; McKerrow, A. J. *Langmuir* **1998**, *14*, 816.

(20) Shirley, D. A. *Phys. Rev. B* **1972**, *5*, 4709.

(21) Rogach, A. L.; Kornowski, A.; Gao, M.; Eychmuller, A.; Weller, H. J. *Phys. Chem. B* **1999**, *103*, 3065.

(22) Rama Krishna, M. V.; Friesner, R. A. *J. Chem. Phys.* **1991**, *95*, 8309.

(23) Landes, C. F.; Braun, M.; El-Sayed, M. A. *J. Phys. Chem. B* **2001**, *105*, 10554.

(24) Zhang, J. J. *Phys. Chem. B* **2000**, *104*, 7239.

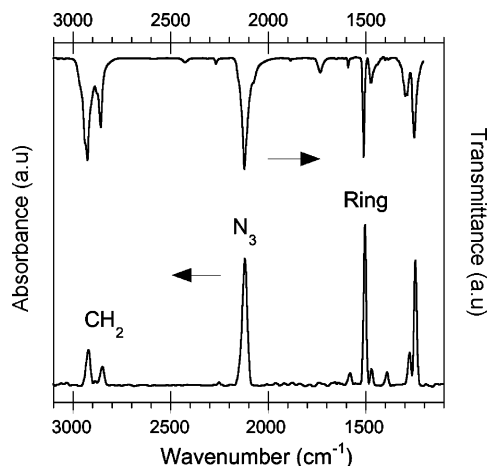


**Figure 2.** FTIR spectra of aryl azide disulfide precursor (transmittance) and aryl azide monolayer on gold (absorbance).

**Table 1. Aryl Azide Disulfide and Aryl Azide SAM FTIR Band Assignment**

assignment	vibration ( $\text{cm}^{-1}$ )	
	bulk	SAM
$\nu_{\text{as}} \text{CH}_2$	2926	2919
$\nu_{\text{s}} \text{CH}_2$	2856	2848
$\text{N}_3$	2122	2117
$(\text{C}=\text{C})_{\text{aryl}}$	1510	1503
$\text{C}-\text{O}$	1250	1245

purity due to the high reactivity of the alkyl azide group. Good coverage and order of the SAMs was observed only when assembly was carried out under argon. FTIR spectra of the disulfide precursor (KBr-transmission) as well as the aryl azide SAM (grazing angle-absorbance) are presented in Figure 2. The significant bands and their assignments are listed in Table 1. The intense peak at  $2117 \text{ cm}^{-1}$  confirms azide presence. The general agreement of the monolayer and bulk precursor IR spectra demonstrates that the structural integrity of the chain and the functional groups is not disturbed by the formation of the monolayer. Finally, based on previous IR studies, the observation of a methylene asymmetric band at  $2919 \text{ cm}^{-1}$  in the SAM (compared to  $2926 \text{ cm}^{-1}$  in the bulk) suggests a densely packed, well-ordered monolayer.<sup>25,26</sup>

SAM integrity was examined further using cyclic voltammetry with the ferrocyanide/ferricyanide couple serving as the redox probe. At a  $100 \text{ mV/s}$  scan rate, dramatic differences in the  $i-E$  response between bare gold and aryl azide monolayer-covered electrodes were observed (Figure 3). A significant drop in cathodic current along with increased peak separation in the case of the aryl azide SAM-coated electrode suggest a transition from a diffusion-limited to a kinetically influenced redox process. This result implies excellent monolayer coverage of the aryl azide-terminated SAM, which substantially inhibits access of the redox probe to the gold electrode surface.

XPS spectra of the aryl azide-terminated SAM further established the presence of the azide functionality and the thiolate bond, and provided a benchmark for comparison after photocatalyzed azide reduction. The N1s photoelectron spectrum is given in Figure 4. Two distinct peaks at 400.5 and 403.8 eV are observed in the detailed scan. The lower binding energy (BE) peak (400.5 eV) is attributed to the electron-rich outer nitrogen(s)

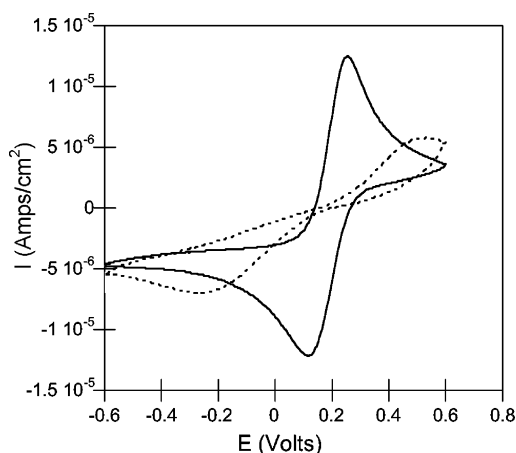


**Figure 3.** Cyclic voltammograms of  $100 \text{ mM K}_4\text{Fe}(\text{CN})_6/\text{K}_3\text{Fe}(\text{CN})_6$  in phosphate buffer before (solid) and after (dotted) gold electrode modification by aryl azide-terminated SAM formation.

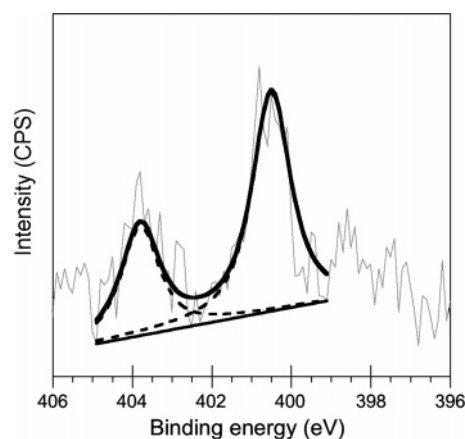


**Figure 4.** XPS N1s photoelectron spectrum of the aryl azide SAM.

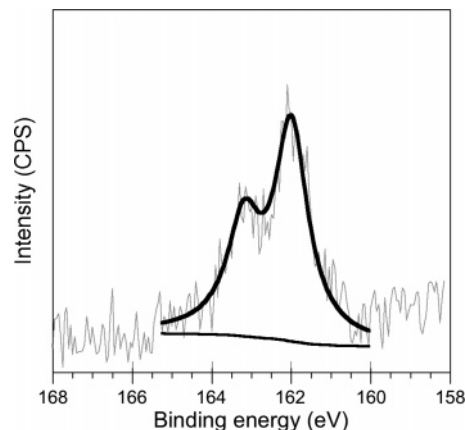


**Figure 5.** XPS S2p photoelectron spectrum of the aryl azide SAM.

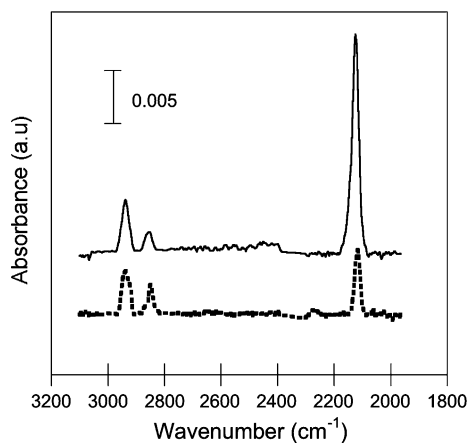
of the azide and the higher BE peak (403.8 eV) to the electron-deficient inner nitrogen.<sup>27</sup> The integrated area of the higher BE peak is half that at the lower BE, as expected based on earlier work.<sup>27</sup>

Figure 5 shows a detailed scan in the 158–170 eV BE range (S2p photoelectron spectra). A characteristic doublet structure is observed. The peak at 162.1 eV is attributed to a  $\text{S}2\text{p}_{3/2}$  photoelectron from the thiolate sulfur. The doublet structure in itself is a consequence of spin–orbit splitting effects, which occur in p and higher orbitals. There is no indication of an oxidized

(25) Snyder, R. G.; Maroncelli, M.; Strauss, H. L.; Hallmark, V. M. *J. Phys. Chem.* **1986**, *90*, 5623.

(26) Porter, M. D.; Bright, T. B.; Allara, D. L.; Chidsey, C. E. D. *J. Am. Chem. Soc.* **1987**, *109*, 3559.

(27) Wollman, E. W.; Kang, D.; Frisbie, C. D.; Lorkovic, I. M.; Wrighton, M. S. *J. Am. Chem. Soc.* **1994**, *116*, 4395.



**Figure 6.** FTIR spectra of the aryl azide SAM before (solid) and after (dotted) 2 h of photocatalytic reduction in a free suspension of CdS QDots (pH 7).

S species ( $\sim 161$  eV) or disulfides ( $\sim 164$  eV), which indicates that the disulfide dissociates and reacts to give a chemisorbed thiolate layer.

**Photocatalytic Reduction with Qdots Initially in Free Suspension.** Apart from redox potentials, heterogeneous charge transfer at the semiconductor–substrate interface also is influenced by Qdot adsorption, electrostatic effects, and site-specific interactions.<sup>28</sup> Without highly favorable Qdot adsorption from free suspension onto the aryl azide SAM, recombination of the excited electron–hole pair would occur faster than electron transfer to the azide, resulting in inefficient azide reduction. Fortunately, excellent CdS Qdot (pH 7.0) adsorption onto the aryl azide SAM was observed. This was confirmed both by XPS and by measurements of adsorbed Qdot luminescence. A detailed XPS spectrum in the 400–416 eV BE range showed the characteristic Cd3d doublet with the Cd3d<sub>5/2</sub> and Cd3d<sub>3/2</sub> peaks at 405.1 and 412.0 eV, respectively. The surface luminescence spectrum also included a characteristically broad peak centered at 550 nm confirming the presence of active Qdots. In fact, the interaction of adsorbed Qdots with the SAM was so strong that they could not be desorbed by rinsing the surface repeatedly with up to 1 M saline or by ultrasonication (without SAM destruction). However, a 6-hour treatment of the SAM in 6 M guanidine hydrochloride freed the SAM surface of Qdots, which was verified by XPS. No Cd3d doublet was observed in the XPS spectrum after guanidine treatment, which suggested complete Qdot desorption. Therefore, in all cases after photocatalytic reduction, the photocatalytically reduced SAMs were cleaned with guanidine hydrochloride solution and subsequently rinsed with water before doing any further SAM characterization.

FTIR, contact angle goniometry, and XPS were used collectively to confirm partial photocatalytic reduction of aryl azide-terminated monolayer to the corresponding arylamine. The FTIR spectrum of the SAM before and after photocatalytic reduction is shown in Figure 6. After a 2-h reduction, there is a significant decrease in the azide band intensity, whereas no significant change was observed in both the asymmetric and symmetric methylene band intensities. Although this result suggested partial azide reduction, no characteristic amine stretches were observed (3500 and 3400  $\text{cm}^{-1}$ ). However, this is not surprising, as amine N–H bonds have weak dipoles. In fact, a commercially available amine thiol with an eleven-carbon alkyl chain was purchased from Dojindo Inc. and was allowed to self-assemble onto a clean gold substrate. No N–H amine stretch was observed in the FTIR

(28) Kamat, P. V. *Prog. React. Kinet.* **1994**, *19*, 277.

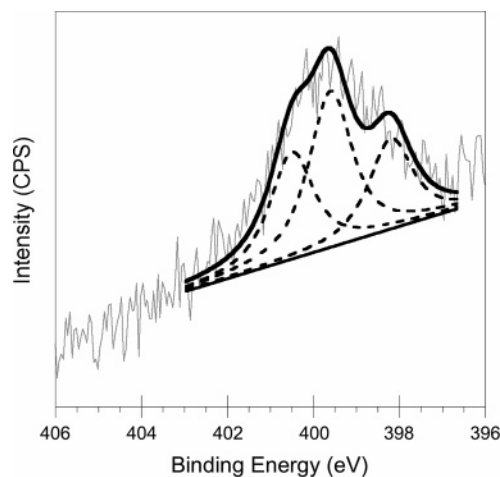


**Figure 7.** XPS N1s spectra of the aryl azide SAM after 2 h of photocatalytic reduction in a solution of CdS quantum dots (pH 7).

spectrum in this case either (data not shown), which supports the contention that terminal amines of SAMs are not detected easily using FTIR.

All of the photocatalytically reduced SAMs also were characterized using contact angle goniometry and XPS to further investigate the reaction and to confirm the presence of arylamine. As an arylamine monolayer should be more hydrophilic than an aryl azide monolayer, static water contact angle measurements were made before and after photocatalytic reduction for comparison. A contact angle of  $78^\circ \pm 2^\circ$  was obtained for the aryl azide SAM, while the contact angle after reduction was found to be  $59^\circ \pm 2^\circ$ . Typical contact angles for amine-terminated monolayers are expected to be  $\sim 43^\circ$ .<sup>29</sup> This difference of  $10^\circ$  is attributed to partial reduction of the starting aryl azide monolayer, which would result in arylamines interspersed with azides at the SAM surface.

The XPS N1s spectrum of a photocatalytically reduced SAM exhibited a rather broad feature centered at 399.5 eV (Figure 7). An amine N1s photoelectron has been reported to give rise to a characteristic single peak at 399.5 eV.<sup>30–33</sup> Three peaks at 399.5, 400.6, and 398.3 eV, respectively, were obtained after deconvolution of the broad feature in the reduced SAM spectrum. The peak at 399.5 eV confirmed arylamine presence. The feature at 400.6 eV is the same peak observed in the starting azide SAM attributed to azide outer nitrogen, confirming partial reduction of the starting azide SAM. The third deconvoluted peak at 398.3 eV is not characteristic of an azide or amine monolayer. Prior reports have attributed an N1s photoelectron peak in the 398–398.5 eV range to either imine nitrogen or nitrogen directly bonded to metal.<sup>30,34</sup> Since the existence of either of these circumstances is unlikely in this case, this peak is believed to arise from direct azide photolysis. It is well-known that azides are photosensitive and can absorb UV light to form unstable and highly reactive singlet nitrenes.<sup>35,36</sup> These nitrenes could potentially react with nearby azides to form more stable products such as tetraazadienes whose N1s photoelectron would have a

(29) Wang, H.; Chen, S.; Li, L.; Jiang, S. *Langmuir* **2005**, *21*, 2633.

(30) Adenier, A.; Chehimi, M. M.; Gallardo, I.; Pinson, J.; Vila, N. *Langmuir* **2004**, *20*, 8243.

(31) Nakagaki, R.; Frost, D. C.; McDowell, C. A. *J. Electron Spectrosc. Relat. Phenom.* **1981**, *22*, 289.

(32) Neoh, K. G.; Kang, E. T. *J. Phys. Chem.* **1992**, *96*, 6777.

(33) Chernyshova, I. V.; Hanumantha Rao, K. *Langmuir* **2001**, *17*, 2711.

(34) Schwaner, A. L.; Pylant, E. D.; White, J. M. *J. Vac. Sci. Technol. A* **1996**, *14*, 1453.

(35) Leyva, E.; Platz, M.; Percy, G.; Wirz, J. *J. Am. Chem. Soc.* **1986**, *108*, 3783.

(36) Schuster, G.; Platz, M. *Adv. Photochem.* **1987**, *17*, 69.

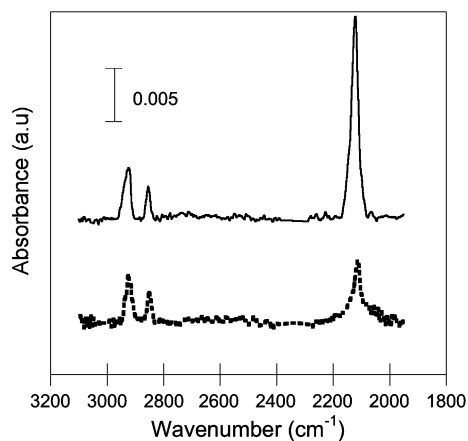


**Figure 8.** FTIR spectra of aryl azide SAM before (solid) and after (dotted) 48 h of chemical reduction with 0.01 M  $\text{Ph}_3\text{P}$  in THF.

lower BE than azide or amine N1s photoelectrons. Nevertheless, XPS data along with contact angle data confirmed partial photocatalytic reduction of aryl azide to the corresponding arylamine monolayer. Increasing photocatalysis time beyond 2 h did not lead to complete or near-complete reduction. We believe that photocatalytic electron transfer occurs only from Qdots adsorbed on the azide moieties and that these adsorbed Qdots lose photocatalytic activity during the course of the experiment. Since Qdots adsorb tightly on the SAM, exchange with fresh Qdots in solution is restricted, and the SAM surface eventually becomes coated with inactive Qdots thereby limiting photocatalytic conversion of the azide.

To support the above evidence of azide to amine photocatalytic reduction, a positive control experiment was carried out. The aryl azide SAM was chemically reduced using triphenylphosphine ( $\text{Ph}_3\text{P}$ ) as the reducing agent.  $\text{Ph}_3\text{P}$  reduction has been reported to selectively reduce azides to the corresponding amines.<sup>37</sup> The same three techniques (i.e., FTIR, contact angle goniometry, and XPS) were used to characterize the  $\text{Ph}_3\text{P}$ -reduced SAM after chemical reduction and subsequent water rinsing. In the first 24 h of reduction, the azide band intensity in the FTIR spectrum dropped to 60% of the starting intensity. After 48 h of reduction, the azide stretch had dropped to 25% in the FTIR spectrum (Figure 8) while the methylene IR band intensity remained unchanged indicating relatively efficient reduction of the starting aryl azide SAM. The contact angle for this reduced SAM was found to be  $51^\circ \pm 1^\circ$ , which is closer to that expected for an amine-terminated monolayer. The XPS N1s spectrum (Figure 9) of the  $\text{Ph}_3\text{P}$  reduced SAM displayed a broad feature as in the case of the photocatalytically reduced SAM, which could be deconvoluted into two independent peaks (399.5 eV, 400.5 eV). This confirmed that the peak at 399.5 eV was indeed from the arylamine and that the 400.5 eV feature is from the unreduced aryl azide.

Ideally, the ratio of the area under the deconvoluted aryl azide and amine N1s peaks (XPS spectrum) should give an estimate of the surface azide to amine conversion. However, these estimates may not be quantitatively accurate, because at neutral pH the arylamine is known to exist as a mixture of both protonated and neutral species,<sup>30,33,38</sup> and the N1s peak for the protonated amine nitrogen has been observed to appear at higher binding energies relative to the neutral amine ( $\sim 401$  eV). The presence of an unreduced azide peak at  $\sim 400.6$  eV in the photocatalytically reduced SAM makes it difficult to deconvolute and resolve the

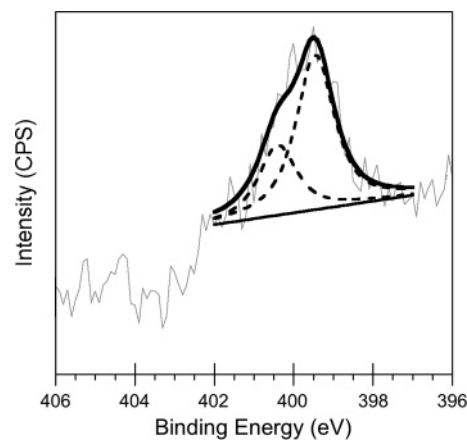


**Figure 9.** XPS N1s spectra of the aryl azide SAM after 48 h of chemical reduction with 0.01 M  $\text{Ph}_3\text{P}$  in THF.

azide and protonated amine N1s peaks. Thus, if the azide and protonated amine N1s photoelectron peaks were to overlap in our case, the conversion would actually be more than what is obtained assuming the presence of neutral arylamine species alone. Such a scenario would also explain the absence of the less intense inner nitrogen azide peak at 403.8 eV, which we believe is lost among the noise in the spectra of SAMs that were either photocatalytically or chemically reduced. Assuming no protonated amine nitrogen, we estimated the aryl azide to arylamine conversion to be  $\sim 47\%$ , which would be the lower conversion limit. In a similar manner, the extent of nonphotocatalytic azide reduction to a speculative tetraazadiene product was estimated at  $\sim 25\%$ .

To complement the positive control experiment, two negative control experiments also were carried out. The photocatalytic reduction protocol described above was repeated without CdS Qdots. In this control, the FTIR spectrum and the contact angle of the SAM before and after the study were found to be almost identical, suggesting no observable change in the nature of the monolayer surface. Also, an XPS N1s spectrum was recorded and deconvoluted. Apart from a strong azide signal, the 398.2 eV peak corresponding to direct photolysis was noted along with a small amine peak ( $< 10\%$  of azide peak intensity). This latter feature is believed to arise from the adsorption of tertiary amine thiol onto the gold substrate at pinhole and other surface defects in the starting azide SAM. Another control consisted of the adsorption of CdS Qdots followed by desorption without photolysis. The FTIR spectra of the SAM before and after the control experiment again were unchanged. These two control experiments suggest that significant azide reduction occurs only upon irradiation in the presence of Qdot photocatalysts.

**Photocatalytic Reduction with Preadsorbed Qdots.** Since Qdots adsorb strongly onto the SAM, photocatalytic reduction was attempted with Qdots preadsorbed by exposure to a dilute solution overnight. In this case, the azide-terminated substrate with adsorbed Qdots was irradiated in sodium formate solution that was free of additional Qdots. After irradiation, the photocatalytically reduced SAM gave rise to a FTIR spectrum with a significantly reduced azide band intensity that had minimal changes in the methylene bands. This is similar to the result described above where freely suspended Qdots were introduced into solution at the time of illumination (Figure 10). The water contact angle on the reduced SAM was determined to be  $61^\circ \pm 2^\circ$  suggesting a more hydrophilic surface relative to the azide SAM. The XPS N1s spectra (Figure 11) was also very similar to that obtained with freely suspended Qdots having a broad feature that was deconvoluted into three separate peaks at 400.5,

(37) Vaultier, M.; Knouzi, N.; Carrie, R. *Tetrahedron Lett.* **1983**, *24*, 763.  
 (38) Shyue, J. J.; De Guire, M. R.; Nakanishi, T.; Masuda, Y.; Koumoto, K.; Sukenik, C. N. *Langmuir* **2004**, *20*, 8693.

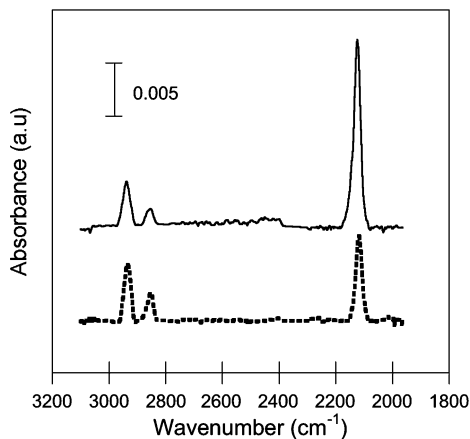


**Figure 10.** FTIR spectra of aryl azide disulfide SAM before (solid) and after (dotted) 2 h of photocatalytic reduction with pre-adsorbed CdS quantum dots (pH 7).

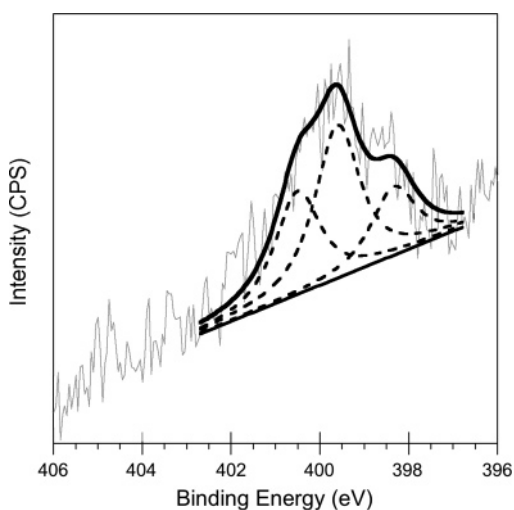


**Figure 11.** XPS N1s spectra of the aryl azide SAM after 2 h of photocatalytic reduction with pre-adsorbed CdS quantum dots (pH 7).

399.6, and 398.2 eV corresponding to azide, amine, and nonphotocatalytic reaction product, respectively. The FTIR, contact angle, and XPS data again confirmed partial reduction of the aryl azide terminal groups on the SAM to the arylamines.

**FITC Derivatization of Arylamine Monolayer.** Derivatization of the terminal arylamine groups of the photocatalytically reduced SAM was carried out successfully with FITC. FITC is known to react with amines in solution to form a stable thiourea product. When excited at around 475 nm, a characteristic emission peak at 520 nm is expected from the derivatized product. The emission spectrum was obtained at 475 nm excitation (Figure 12) and showed a broad peak centered at 520 nm confirming the presence of the fluorescent thiourea product. A control experiment was carried out where an aryl azide SAM sample was exposed to FITC under the same conditions. No fluorescent tagging was

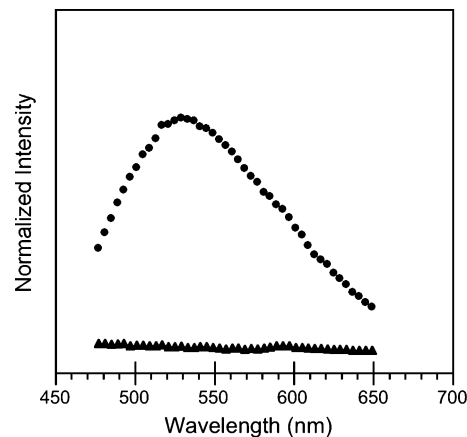


**Figure 12.** Emission spectra of CdS Qdot reduced arylamine monolayer derivatized with FITC (●) and a control aryl azide monolayer (▲).

observed. It is of interest that the excited-state emission does not seem to be quenched by the underlying gold substrate.<sup>39</sup> This might be due to the combined effect of covalent coupling of the fluorophore and the ten-carbon alkyl chain backbone, which may provide dielectric shielding.

### Concluding Remarks

A tightly packed, ordered aryl azide-terminated SAM was self-assembled on a gold surface from a new aryl azide disulfide precursor. Partial reduction of the aryl azide-terminated monolayer to the corresponding arylamine was accomplished using ~2-nm-diameter CdS Qdots as photocatalysts with an irradiation time of 2 h. The reduced monolayer was derivatized by covalently tagging the arylamine with FITC. This work could lead to a facile method to create pre-defined amine nanopatterns against an azide background by selective adsorption of Qdots on an azide-terminated SAM surface followed by photocatalytic reduction. Such Qdot photocatalyzed chemical nanopatterning on azide-terminated SAMs currently is under investigation.

**Acknowledgment.** This research was funded by the MARCO Functional Engineered Nano Architectonics (FENA) Center, part of the Focus Center Research Programs (FCRP). We thank Prof Garrell (UCLA Chemistry and Biochemistry) for access to the FTIR and contact angle equipment, and Dr. Tom Mates for help with XPS (MRL Central Facilities supported by the MRSEC Program of the National Science Foundation under Award No. DMR00-80034).

**Supporting Information Available:** Aryl azide disulfide precursor synthesis procedures and analytical and spectral characterization data. This material is available free of charge via the Internet at <http://pubs.acs.org>.

LA060035Y

(39) Whitmore, P. M.; Robota, H. J.; Harris, C. B. *J. Chem. Phys.* **1982**, *77*, 1560.